Combined BER Analysis for Time-Frequency Synchronization Schemes for MB-OFDM UWB

Debarati Sen, *Member, IEEE*, Saswat Chakrabarti, *Member, IEEE,* and R. V. Raja Kumar, *SM, IEEE*

***Abstract*— In this paper we present the closed form expression of bit-error-rate (BER) of a convolution coded MB-OFDM Ultra-Wideband (UWB) system. The analysis considers the log-normal fading statistics of UWB channels and captures the estimation error variances of timing and carrier frequency offset (CFO) estimation by our already published synchronizers[1] ATS [1] and MBAFS [2] respectively. The derivation invokes moment generating function (MGF) for log-normal fading statistics and the Gauss-Hermite quadrature integration to deliver average BER expression for rate R_c coded QPSK modulated MB-OFDM system with ATS and MBAFS synchronizers and least square (LS) channel estimator. The analytical result is validated with simulation in the high delay spread UWB channel model CM3. This analysis helps in thorough understanding on the performance of an OFDM based communication system in an Ultra-Wideband environment.**

***Index Terms*—BER; UWB; synchronization**

I. Introduction

Mathematical analysis of bit-error-rate (BER) performance bound for coded MB-OFDM Ultra-Wideband (UWB) system with synchronization schemes under realistic UWB channel has immense importance. In this paper, we obtain approximate and simple analytical expression of BER considering a binary convolution code with soft Viterbi algorithm using our earlier proposed synchronization schemes ATS [1] and MBAFS [2] in the receiver. The derivation associates moment generating function (MGF) as the key analytical tool. We put emphasis on useful assessment of BER performance and compare with our simulation results to validate the analysis.

The analysis is carried out in three steps: deriving the average BER for uncoded system considering log-normal fading statistics, with ideal synchronization and channel estimation; then, convolution coding is incorporated to obtain BER expression for ideal timing, frequency, and channel estimation; finally, the BER is derived for a convolution coded MB-OFDM system which involves timing correction by ATS method, frequency synchronization by MBAFS method, and channel estimation by least square (LS) error method. The analytical results are verified through simulation. For simplicity of analysis, the shadowing effect of the channel is excluded and the statistically independent log-normal distributed multipath gain coefficients are considered.

Rest is organized as follows: Section II presents the BER analysis for uncoded system, convolution coded system with ideal synchronization, and with synchronization errors. Section III briefs about simulation results and discussions. Section IV concludes our study with the summary.

Debarati Sen is presently with the Department of Signals and Systems, Chalmers University of Technology, Gothenburg, Sweden (e-mail: debarati@chalmers.se; phone: +46 31 772 1885). During this work she was associated with the G. S. S. School of Telecommunications, Indian Institute of Technology Kharagpur, India.

Saswat Chakrabarti is with the G. S. S. School of Telecommunications, Indian Institute of Technology Kharagpur, India.

R. V. Raja Kumar is presently with the R. G. University of Knowledge Technologies, Hyderabad, India. During this work he was associated with the Department of E&ECE, Indian Institute of Technology Kharagpur, India.

[1] Due to page limitations, readers are requested to follow reference [1] and [2] for our earlier proposed timing synchronizer ATS and frequency synchronizer MBAFS.

II. BER Analysis

A. Uncoded System

We analyze the system in WPAN environment where channel is expected to be slowly varying. The fading statistics governs the probability density function (PDF) of the instantaneous SNR per bit (γ) which is a time invariant random variable. The average BER is given by

$$P_e = \int_0^\infty Q\left(a\sqrt{\gamma}\right) P_\gamma(\gamma) \tag{1}$$

where, a depends on modulation/detection combination and is constant. The classical definition of Gaussian Q-function $Q(x) = \int_x^\infty \left(1/\sqrt{2\pi}\right)\exp\left(-y^2/2\right)dy$ suffers from two disadvantages: a) for computation this requires truncation of upper infinite limit when using numerical integral evaluation, b) the presence of argument of the function as lower limit of the integral poses analytical difficulties when this argument depends on another random parameter that requires statistical average of their probability distributions. We use the alternative definition of Q-function defined by Simon *et al.* [3]

$$Q(x) = \frac{1}{\pi}\int_0^{\pi/2} \exp\left(-x^2/2Sin^2\theta\right)d\theta \quad \text{for } x \geq 0 \tag{2}$$

The above definition of Q-function has finite integration limits which are independent of the argument of function x and the integrand has a Gaussian form with respect to x. The derivation of Eq. (2) from the classical definition of Q-function is given in [3].

Substituting Eq. (2) in Eq. (1) the average BER leads to

$$P_e = \frac{1}{\pi}\int_0^{\pi/2}\left\{\int_0^\infty \exp\left(-a^2\gamma/2Sin^2\theta\right)P_\gamma(\gamma)\,d\gamma\right\}d\theta \tag{3}$$

The inner integral within the bracket of Eq. (3) can be expressed in terms of moment generating function (MGF) defined as [3]

$$M_\gamma(s) \triangleq \int_0^\infty e^{s\gamma} P_\gamma(\gamma)\, d\gamma \tag{4}$$

So, average BER (Eq. (3)) in terms of MGF is expressed as

$$P_e = \frac{1}{\pi}\int_0^{\pi/2} M_\gamma\left(-a^2/2Sin^2\theta\right) d\theta \tag{5}$$

The UWB channel shows log-normal fading with PDF as

$$P_\gamma(\gamma) = \left\{(10/\ln(10))/\sqrt{2\pi\sigma^2\gamma}\right\} \exp\left[-(10\log_{10}\gamma - \mu)^2/2\sigma^2\right] \tag{6}$$

Here, μ (dB) and σ (dB) are respective mean and standard deviation of $10\log_{10}\gamma$. MGF corresponding to log-normal distribution is obtained by substituting Eq. (6) in Eq. (4) and using the Gauss-Hermite quadrature integration [3, Eq. (25.4.46)] for the inner integral in Eq. (4) as follows:

$$M_\gamma(-s) = \frac{1}{\sqrt{\pi}} \sum_{n=1}^{N_p} H_{x_n} \exp\left[10^{\left(\sqrt{2}\sigma x_n + \mu\right)/10} s\right] \tag{7}$$

where $\{x_n\}$, n = 1, 2, …, N_p are the zeros of the N_p -th order Hermite polynomial $He_{N_p}(x)$ and $\{H_{x_n}\}$; n = 1, 2, ……, N_p are corresponding weight factors tabulated in Table 25.10 of [4] for values of N_p from 2 to 20.

ECMA-368 [5] for MB-OFDM recommends both QPSK and Dual Carrier Modulation (DCM). We consider QPSK modulation for our analysis. For uncoded system, average BER with QPSK modulation from Eq. (5) is as [6, pp. 141]

$$P_e = \frac{1}{\pi}\int_0^{3\pi/4} M_\gamma\left(-a^2/2Sin^2\theta\right) d\theta \;;\; a^2 = 2\sin^2\pi/M \tag{8}$$

Substituting the MGF for log-normal fading from Eq. (7) into Eq. (8), average BER for uncoded system with QPSK modulation and log-normal faded channel under ideal time, frequency and channel estimation converges to

$$P_e = \frac{1}{\pi^{3/2}} \sum_{n=1}^{N_p} H_{x_n} \int_0^{3\pi/4} \exp\left[-10^{\left(\sqrt{2}\sigma x_n + \mu\right)/10} \left(E_b/N_0\right)\left(1/2\sin^2\theta\right)\right] d\theta$$

$$\text{where,} \quad \gamma = E_b/N_0 \tag{9}$$

Equation (9) allows evaluation of bit error probability in simple way as it involves a single integral on θ and values of $\{x_n\}$ and $\{H_{x_n}\}$ can be substituted from Table 25.10 of [4]. Our BER analysis for coded system with ideal synchronization and proposed synchronizers is based on Eq. (9). We do analysis for convolution coded system below.

B. Convolution Coded System with Ideal Synchronization

We now proceed our BER analysis further for convolution coded QPSK modulated MB-OFDM system considering perfect timing and frequency synchronization.

Suppose that transmitted bits are encoded by a convolution encoder CC (*k*, *n*) and interleaved with a depth exceeding coherence time of channel. The sequence is bit-wise interleaved to ensure that bits in any code word fade independently. A soft Viterbi decoder in conjunction with coherent demodulator retrieves the information at the receiver.

Using union bound arguments [7], the bit error probability of a convolution code with code rate R_{cc} (= *k*/*n*) can be upper bounded by

$$P_b < \sum_{\tilde{d}=d_{free}}^{\infty} c_{\tilde{d}}\, P_{\tilde{d}} \tag{10}$$

Here, $P_{\tilde{d}}$ is pair-wise error probability with Hamming distance $\tilde{d}$, $c_{\tilde{d}}$ is sum of bit errors (information error weight) for events of distance $\tilde{d}$, and d_{free} is free distance of the code. For simplification, we assume that Hamming distances $\tilde{d}$ are mutually independent to each other. This leads to calculate the pair-wise error probability $P_{\tilde{d}}$ using the error probability expression for *L*-diversity reception with maximum ratio combining for identically distributed fading for all channels with QPSK modulation scheme [6, Section 9.2] may be given as

$$\tilde{P}_e = \frac{1}{\pi}\int_0^{3\pi/4} \left(M_\gamma\left(-1/\sin^2\phi\right)\right)^L d\phi \tag{11}$$

Following Eq. (11) the pair-wise error probability $P_{\tilde{d}\_ideal}$ for convolution coded (at rate R_{cc}) QPSK modulated bits transmitted over log-normal fading channel and decoded by soft Viterbi decoder with ideal synchronization parameter (timing and frequency) estimation is obtained by Eq. (9) as

$$P_{\tilde{d}\_ideal} = \frac{1}{\pi}\int_0^{3\pi/4} \left\{\frac{1}{\sqrt{\pi}} \sum_{n=1}^{N_p} H_{x_n} \exp\left[-10^{\left(\sqrt{2}\sigma x_n + \mu\right)/10} R_{cc} \frac{E_b}{N_0}\left(a^2/2\sin^2\theta\right)\right]\right\}^{\tilde{d}} d\theta \tag{12}$$

As the zeros of Hermite polynomial H_{x_n} are independent of θ, the above expression can be rewritten as

$$P_{\tilde{d}\_ideal} = \frac{1}{\pi}\left(\frac{1}{\sqrt{\pi}}\right)^{\tilde{d}} \sum_{n=1}^{N_p} H_{x_n} \int_0^{3\pi/4} \left\{\exp\left[-10^{\left(\sqrt{2}\sigma x_n + \mu\right)/10} R_{cc}\left(E_b/N_0\right)\left(a^2/2\sin^2\theta\right)\right]\right\}^{\tilde{d}} d\theta \tag{13}$$

In deriving Eq. (13) we have assumed that channel is slow fading and channel state information (CSI) is known. The noise power N_0 is the contribution of AWGN with mean zero and variance σ^2_{awgn}. Substituting Eq. (13) in Eq. (10) the upper bound of BER P_{b_ideal} with ideal parameter estimation of channel, timing and frequency is obtained as

$$P_{b\_ideal} < \sum_{\tilde{d}=d_{free}}^{\infty} c_{\tilde{d}} P_{\tilde{d}\_ideal} \quad (14)$$

Equation (14) is plotted in Fig. 1 to verify with simulation results. As the pair-wise error probability $P_{\tilde{d}\_ideal}$ for fading channel decreases slower than the AWGN case $\left(P_{\tilde{d}} = Q\sqrt{2\tilde{d}R_{cc}\left(E_b/N_0\right)}\right)$, the information error weight $c_{\tilde{d}}$ will have larger influence on BER. So, we need to choose a CC which performs well on both AWGN and fading channel, and has maximum free distance with low information error weight on each error path. We have chosen the matching error weights of optical distance spectrum (ODS) CC given in [8]. Considering UWB channel is less severe than Rayleigh fading channel [9], and due to unavailability of error weights for log-normal fading channel, we have used error weights $c_{\tilde{d}}$ of Rayleigh fading from [8] to plot Eq. (14). Next, we derive the BER expression incorporating timing and frequency estimation error variances.

C. Convolution Coded System with Synchronization Errors

The estimation errors of timing and frequency will contribute to inter-carrier-interference (ICI) which controls the BER performance. For the ease of analysis we exclude the effect of imperfect channel equalization.

Let, the residual frequency offset (RFO) after CFO estimation by MBAFS be $\delta\varepsilon$ and timing jitter for *n*-th sample after timing synchronization by ATS be $\delta\tau(n)$. We evaluate the ICI powers for both the residual errors separately. Let, each sub-carrier has signal power of σ_s^2. Assume that signal power in a specific sub-carrier, ICI power from other sub-carriers due to residual time-frequency errors, and additive noise are mutually uncorrelated. The impact of ICI due to time-frequency offsets on a sub-carrier from all other sub-carriers is modeled as zero mean Gaussian random variable.

Case 1 : Effect of RFO under the Assumption of Perfect Timing Estimation

First, we compute the ICI power due to RFO $\delta\varepsilon$ due to CFO estimation error of MBAFS algorithm considering perfect timing estimation. For the system model in [2], sampled signal for the *k*-th sub-carrier after CFO synchronization by MBAFS and FFT processing at the receiver is

$$Y(k) = S(k)H(k)I_{\delta\varepsilon}(0) + \underbrace{\sum_{l\neq k, l=0}^{N-1} S(l)H(l)I_{\delta\varepsilon}(l-k)}_{ICI_{\delta\varepsilon}} + W(k) \quad (15)$$

Here, $k = 0...N-1$, $S(k)$ is transmitted symbol on *k*-th sub-carrier, $H(k)$ is *k*-th sample of channel frequency response, $I_{\delta\varepsilon}(0)$ is attenuation of *k*-th sub-carrier due to RFO, and $W(k)$ is additive white Gaussian noise with variance σ_{awgn}^2. Second term in Eq. (15) is ICI due to RFO $\delta\varepsilon$ given as [10]

$$I_{\delta\varepsilon}(l-k) = \frac{\sin\pi(l-k+\delta\varepsilon)}{N\sin\frac{\pi}{N}(l-k+\delta\varepsilon)} \exp\left[\frac{j\pi(N-1)}{N}(l-k+\delta\varepsilon)\right] \quad (16)$$

The corresponding ICI power can be shown as

$$\sigma_{\delta\varepsilon}^2(k) = \sigma_s^2 \sum_{l=0, l\neq k}^{N-1} |H(l)|^2 \frac{\sin^2\pi(l-k+\delta\varepsilon)}{N^2\sin^2\frac{\pi}{N}(l-k+\delta\varepsilon)} \quad (17)$$

So, the average SNR of the *k*-th sub-carrier due to residual CFO under perfect timing synchronization is obtained as

$$\bar{\gamma}_{\delta\varepsilon}(k) = \left\{\sigma_s^2 |H(k)|^2 |I_{\delta\varepsilon}(0)|^2\right\} \Big/ \left\{\sigma_{\delta\varepsilon}^2 + \sigma_{awgn}^2\right\} \quad (18)$$

where $I_{\delta\varepsilon}(0)$ is obtained as $I_{\delta\varepsilon}(0) = \sin(\pi\delta\varepsilon)/N\sin(\pi\delta\varepsilon/N)$ by substituting $l = k$ in the expression (15).

Case 2 : Effect of Timing Jitter under the Assumption of Perfect Frequency Offset Estimation

Assuming frequency estimation is perfect, the ICI due to timing algorithm ATS is evaluated. Let, after timing synchronization the timing jitter for *n*-th sample is $\delta\tau(n)$. We assume $\delta\tau(n)$ as a wide sense stationary Gaussian random process with zero-mean and variance σ_τ^2. So, *n*-th received sample with timing jitter may be shown as

$$y(n) = \frac{1}{N}\sum_{k=0}^{N-1} S(k)H(k)e^{\frac{-j2\pi(n+\delta\tau(n))k}{N}} + w(n) \quad (19)$$

Here, $n = 0,1,..N-1$. It is known that the timing jitter at adjacent samples in the receiver becomes more correlated when sampling rate increases. To generalize our analysis, we incorporate correlation coefficient ρ_{n-p} between $\delta\tau(n)$ and $\delta\tau(p)$. For Gaussian correlation, ρ_{n-p} can be expressed as [11] $\rho_{n-p} = e^{-\beta^2(n-p)^2}$. Later on, we have computed the ICI power considering white timing jitter with appropriate conditioning of ρ_{n-p}. After FFT of Eq. (19) the received sample on the *m*-th sub-carrier can be expressed as

$$Y(m) = \sum_{n=0}^{N-1} y(n)e^{\frac{j2\pi nm}{N}} + W(m); \qquad (m = 0,1,.....N-1)$$

$$= \sum_{k=0}^{N-1} S(k)H(k)\frac{1}{N}\sum_{n=0}^{N-1} e^{\frac{j2\pi n}{N}(k-m)} e^{\frac{j2\pi k\delta\tau(n)}{N}} + W(m) \quad (20)$$

Expression (20) can be divided into three parts:

$$Y(m) = I_{\delta\tau}(0)\hat{S}(m) + \underbrace{I(m)}_{ICI_{\delta\tau}} + W(m) \quad (21)$$

Where the first term is the desired part phase rotated by

coefficient $I_{\delta\tau}(0)$ given as

$$I_{\delta\tau}(0)=\frac{1}{N}\sum_{n=0}^{N-1}e^{\left(j2\pi m\delta\tau(n)/N\right)} \tag{22}$$

$I_{\delta\tau}(0)$ is a small error vector in the complex plane indicating the effect of residual timing error on the desired sub-carrier. $|I_{\delta\tau}(0)|$ is a random variable and is assumed that the mean value of its magnitude is 1.0. The desired part in Eq. (20) is also attenuated in magnitude due to timing jitter [12] by $\{\sin\pi(m\delta\tau)\}/\{N\sin(\pi/N)(m\delta\tau)\}$. Here, the effect of this amplitude reduction is neglected assuming that its value will be very small after synchronization by ATS.

The second term in equation (21) creates the ICI may be given as

$$I(m)=\sum_{\substack{k=0,\\k\neq m}}^{N-1}S(k)H(k)\left\{\frac{1}{N}\sum_{n=0}^{N-1}e^{\frac{j2\pi n}{N}(k-m)}e^{\frac{j2\pi k\delta\tau(n)}{N}}\right\} \tag{23}$$

It is noticeable from equations (22) and (23) that in the absence of timing jitter i.e., for $\delta\tau(n)=0$, $I(0)$ becomes unity and the ICI term $I(m)$ vanishes as expected. Now, the average ICI power can be computed from Eq. (23) as

$$\sigma_{\delta\tau}^2=E\left\{|I(m)|^2\right\}=E\left\{\left|\sum_{\substack{k=0,\\k\neq m}}^{N-1}S(k)H(k)\left(\frac{1}{N}\sum_{n=0}^{N-1}e^{\frac{j2\pi n}{N}(k-m)}e^{\frac{j2\pi k}{N}\delta\tau(n)}\right)\right|^2\right\}$$

$$=\frac{\sigma_S^2}{N^2}\sum_{k\neq m}|H(k)|^2\sum_n\sum_p e^{\frac{j2\pi}{N}(n-p)(k-m)}e^{\frac{-4\pi^2k^2\sigma_\tau^2}{N^2}\left(1-\rho_{n-p}\right)} \tag{24}$$

Now, considering the timing jitter to be white, the correlation coefficient is given as

$$\rho_m=\begin{cases}1, & \text{when } m=0\\ 0, & \text{when } m\neq 0\end{cases} \tag{25}$$

In the presence of white timing jitter, where $\rho_{n-p}=0$, using Taylor series expansion for the exponential term in Eq. (24) while omitting the second and higher order terms and using following approximation for small values of θ_l: $e^{-j\theta_l}\approx 1-j\theta_l$, the average ICI power can be obtained as

$$\sigma_{\delta\tau}^2=\frac{\sigma_S^2}{N}\sum_{k\neq m}|H(k)|^2\left(1-e^{\left(-4\pi^2k^2\sigma_\tau^2/N^2\right)}\right) \tag{26}$$

For large number of sub-carriers N, the ICI power due to timing jitter can be approximated to [13]

$$\sigma_{\delta\tau}^2\approx\sigma_S^2\sum_{k\neq m}|H(k)|^2\sigma_\tau^2 \tag{27}$$

Case 3 : Effect of Timing Jitter, RFO Error and AWGN

In practice, after timing and frequency synchronization the ICI powers given by equations (27) and (17) will control the BER performance of the system. Hence, in presence of residual frequency error $\delta\varepsilon$ and timing jitter $\delta\tau(n)$, the best possible k-th sub-carrier amplitude at the output of FFT processor after frequency and timing offset corrections may be approximated following Eq. (15) and (21) as

$$Y(k)=S(k)H(k)I_{\delta\varepsilon,\delta\tau}(0)+ICI_{\delta\varepsilon}+ICI_{\delta\tau}+W(k) \tag{28}$$

where, $I_{\delta\varepsilon,\delta\tau}(0)$ signifies the magnitude attenuation and phase rotation of the desired signal due to RFO and timing jitter. Assuming constant timing jitter $\delta\tau$ and RFO $\delta\varepsilon$, $I_{\delta\varepsilon,\delta\tau}(0)$ can be evaluated following Eq. (16) and using Eq. (22) with magnitude attenuation effect as [12]

$$I_{\delta\varepsilon,\delta\tau}(0)=\frac{\sin\pi(\delta\varepsilon+k\delta\tau+\delta\varepsilon\delta\tau)}{N\sin\frac{\pi}{N}(\delta\varepsilon+k\delta\tau+\delta\varepsilon\delta\tau)}\exp\left[\frac{j\pi(N-1)}{N}(\delta\varepsilon+k\delta\tau+\delta\varepsilon\delta\tau)\right] \tag{29}$$

It is noticeable from Eq. (29) that when only residual CFO is present, i.e. $\delta\tau=0$, the phase shift [i.e. the exponent in Eq. (29)] is independent of sub-carrier index k and is identical in every sub-carrier. But, when only timing jitter is present, i.e. $\delta\varepsilon=0$, the phase shift is proportional to the sub-carrier index k as well as the timing jitter itself.

Under the assumption that both ICI power and noise power are independent to each other, the average SNR of k-th sub-carrier in presence of both residual time-frequency errors may be obtained using equations (28) with appropriate substitutions from (17), (27), and (29) as

$$\bar{\gamma}_{\delta\varepsilon,\delta\tau}(k)=\left\{\sigma_s^2|H(k)|^2|I_{\delta\varepsilon,\delta\tau}(0)|^2\right\}/\left\{\sigma_{\delta\varepsilon}^2+\sigma_{\delta\tau}^2+\sigma_{awgn}^2\right\} \tag{30}$$

where $\sigma_{\delta\varepsilon}^2$ and $\sigma_{\delta\tau}^2$ are obtained from Eq. (17) and (27) respectively, $|I_{\delta\varepsilon,\delta\tau}(0)|^2$ can be computed from Eq. (29). To calculate the average SNR per bit, $\left(E_b/N_0\right)\big|_{\delta\varepsilon,\delta\tau}$ the Eq. (29) is scaled by the factor $1/\log_2 M$, where M = 4 for QPSK modulation. Assuming perfect CSI (σ_{ce}^2=0) and substituting SNR per bit with proper scaling of Eq. (30), pair-wise error probability P_{d_sync} for convolution coding with synchronization is evaluated from Eq. (13) as

$$P_{d\_sync}=\frac{1}{\pi}\left(\frac{1}{\sqrt{\pi}}\right)^{\tilde{d}}\sum_{n=1}^{N_p}H_{x_n}\int_0^{3\pi/4}\left\{\exp\left[-10^{\left(\sqrt{2}\alpha x_n+\mu\right)/10}R_{cc}\frac{E_b}{N_0}\Big|_{\delta\varepsilon,\delta\tau}\frac{d^2}{2\sin^2\theta}\right]\right\}^{\tilde{d}}d\theta \tag{31}$$

Hence, the simplified BER with timing and frequency synchronization is obtained following Eq. (14) as

$$P_{b\_sync} < \sum_{\tilde{d}=d_{free}}^{\infty} c_{\tilde{d}} P_{\tilde{d}\_sync} \quad (32)$$

We plot the above analytical expressions (14) and (32) in Section III and verify with simulation results. As discussed earlier, we consider the error weights from Ref. [8].

III. Simulation results for combined ATS and MBAFS

A. Simulation Environment

The simulation considers MB-OFDM system with rate-half unpunctured convolution coding and QPSK modulation. The generator polynomial of rate-half convolution code is 133,171 with constraint length k = 7. OFDM symbols are transmitted over 3 frequency bands of band group 1 using TFI pattern 1. IEEE 802.15.3a CM3 is used as propagation medium. In the receiver timing instant of OFDM symbols in each band is estimated and corrected separately using ATS. Timing synchronization is followed by frequency synchronization using MBAFS algorithm. Simulation is carried out for 100,000 noisy realizations under UWB fading channel. We perform channel estimation in each band separately during channel estimation sequences of the frame format by LS method. Relevant parameters are chosen from Table 1.

B. Bit-Error-Rate (BER) Performance

The theoretical and simulated BER performance without and with synchronization errors are shown in Fig. 1. The theoretical results are plotted using analytical expressions (14) and (32) with proper substitution from equations (18) and (30) after scaling by the factor $1/\log_2 M$. The error weights $c_{\tilde{d}}$ considered for the same are given in Table 2 [8].

Further, Eq. (14) is plotted considering d_{free}=10 and evaluating the summation up to Hamming distance $\tilde{d}$ = 20. The zeros $\{x_n\}$ and weight factors $\{H_{x_n}\}$ of Hermite polynomial are obtained from Table 25.10 of [4] for values of N_p from 2 to 20.

The analytical expression (32) is plotted considering perfect CSI i.e. σ_{ce}^2 = 0 for two different conditions: i) with only ICI due to residual frequency estimation error and AWGN i.e. $\sigma_{\delta\tau}^2$ = 0, $\sigma_{\delta\varepsilon}^2$ ≠ 0, substituting the Eq. (18) into Eq. (32) with proper scaling, and ii) with ICI due to both the timing jitter and residual carrier frequency estimation error along with AWGN i.e. $\sigma_{\delta\tau}^2$ ≠ 0, $\sigma_{\delta\varepsilon}^2$ ≠ 0, substituting the Eq. (30) into Eq. (32) with proper scaling. All the analytical results are verified through simulation where timing and frequency are estimated by ATS and MBAFS algorithm and channel is estimated through LS estimate.

TABLE 1: PARAMETERS CONSIDERED FOR MBAFS PERFORMANCE

Parameter	Consideration
Time Frequency Code	1
Preamble Mode	standard
Data Rate	320Mbps
Code Rate	1/2
Time and Frequency domain spreading	no
Data carriers in one OFDM symbol	100
Pilot carriers in one OFDM symbol	12
Number of modulated bits/OFDM symbol	200
Number of OFDM symbols considered for frequency estimation	2, 3, 6
UWB Channel Model	CM1-CM4
Normalized Frequency Offsets	0.033 (band 1) 0.038 (band 2) 0.043 (band 3)

TABLE 2 : ERROR WEIGHTS $c_{\tilde{d}}$ VALUES FOR HAMMING DISTANCES

Hamming distance	$c_{\tilde{d}}$	Hamming distance	$c_{\tilde{d}}$
1	36	11	502690
2	0	12	0
3	221	13	3322763
4	0	14	0
5	1404	15	21292910
6	0	16	0
7	11633	17	134365911
8	0	18	0
9	77433	19	843425871
10	0	20	0

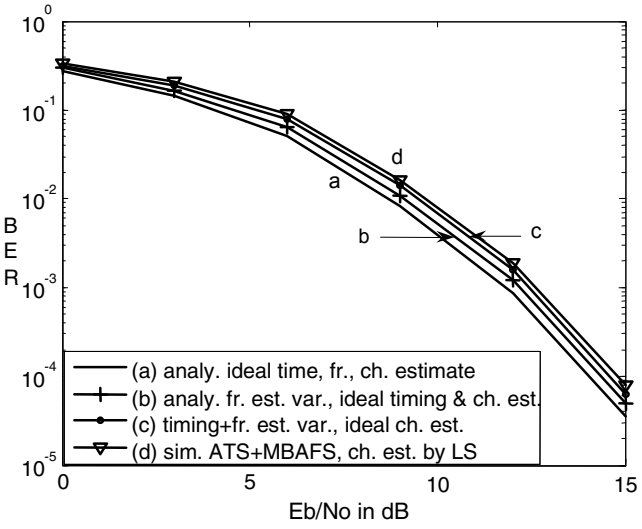

Fig. 1: BER vs. E_b/N_0 for coded MB-OFDM in CM3 for: a) analysis with perfect estimation; b) analysis with frequency estimation error; c) analysis with frequency and timing estimation error; d) simulation with timing, frequency, and channel estimation error.

In Fig. 1 plot (a), plot (b), and plot(c) are the analytical results obtained from analytical expression (14); Eq. (32) with ideal timing and channel estimation (i.e. $\sigma^2_{\delta\varepsilon} \neq 0$); and Eq. (32) with timing and frequency estimation by ATS and MBAFS algorithms considering ideal channel estimation (i.e. $\sigma^2_{\delta\tau} \neq 0$, $\sigma^2_{\delta\varepsilon} \neq 0$) respectively. Simulation result with parameter estimation is plotted as plot (d).

C. Discussions

The BER performance with perfect CSI and ideal synchronization (plot a) is slightly superior than analytical result with only frequency offset estimation and correction (plot b). This is due to the mean-squared-error (MSE) of frequency estimation algorithm.

Plot (c) is even inferior to plot (b) as it depicts the analytical BER for residual timing and frequency estimation errors assuming perfect channel estimate. It is interesting to note that the BER obtained through simulation and analysis, plot (d) and plot (c) are consistent and close to each other. The channel estimation error incorporated in simulation but not in analysis signifies the negligible difference between two curves in the figure.

IV. Conclusions

We provide the BER analysis of a convolution coded MB-OFDM system with realizable timing and frequency synchronization algorithms. The log-normal fading statistics of UWB channels is captured and the estimation error variances of timing and CFO estimation by our earlier proposed synchronizers ATS and MBAFS are considered. Derivation invokes the moment generating function (MGF) as analytical tool and uses Gauss-Hermite quadrature integration to obtain closed form average BER expression for rate R_{cc} coded QPSK modulated MB-OFDM system with our earlier proposed synchronization algorithms and a least square channel estimator. The validity of analysis is confirmed through simulation results.

V. Acknowledgement

We would like to acknowledge funding from VINNOVA within the IKT grant 2007-02930 for publication of this paper.

References

[1] D. Sen, S. Chakrabarti, R. V. Raja Kumar, "A Multi-Band Timing Estimation and Compensation Scheme for Ultra-Wideband Communications," *IEEE Globecom-2008*, LA, USA, pp. 1-5, Nov. 30-Dec. 04, 2008.

[2] D. Sen, S. Chakrabarti, R. V. Raja Kumar, "An Improved Frequency Offset Estimation Algorithm by Multi-Band Averaging Method for MB-OFDM based UWB Communication for WPAN Applications," *IEEE ANTS-2008*, Bombay, India, pp. 1-3, Dec. 15-17, 2008.

[3] M. K. Simon, M-S. Alouini, "Digital Communication over Fading Channel," John Wiley, NJ, USA, 2005.

[4] M. Abramowitz, I. A. Stegun, "Handbook of Mathematical Functions with Formulas, Graphs, and Mathematical Tables," 10th Printing, Dover Publications, NY, USA, 1972.

[5] Standard ECMA-368, "High Rate Ultra Wideband PHY and MAC Standard," 3rd Edition - Dec. 2008, Available at: <http://www.ecma-international.org/publications/standards/Ecma-368.htm>.

[6] "Introduction to physical layer specifications of MB-OFDM UWB proposal" Available at: <http://wise.cm.nctu.edu.tw/wise_lab/course/Seminar/Download%20files/MB_OFDM_UWB.pdf>, Sept. 22, 2004.

[7] J. G. Proakis, "Digital Communications," 4th Edition. McGraw Hill International Edition, New York, USA, 2001.

[8] P. Frenger, P. Orten, T. Ottosson, "Convolutional codes with Optimum distance Spectrum," *IEEE Communications Letters*, vol. 3, no. 11, pp. 317–319, Nov. 1999.

[9] H. Q. Lai, W. P. Siriwongpairat, K. J. R. Liu, "Performance analysis of multiband OFDM UWB systems with imperfect synchronization and intersymbol interference," *IEEE Journal on Selected Areas in Communications*, vol. 1, no. 3, pp. 521–534, Oct. 2007.

[10] P. H. Moose, "A technique for orthogonal frequency division multiplexing frequency offset correction," *IEEE Transactions on Communications*, vol. 42, no. 10, pp. 2908-2914, Oct. 1994.

[11] A. V. Balakrishnan, "On the problem of time jitter in sampling," *IEEE Transactions on Information Theory*, vol. 8, no. 3, pp. 226–236, April 1962.

[12] P.-Y. Tsai, H.-Y. Kang, T.-D. Chiueh, "Joint weighted least-squares estimation of carrier-frequency offset and timing offset for OFDM systems over multipath fading channels," *IEEE Transactions on Vehicular Technology*, vol. 54, no. 1, pp. 211–223, Jan. 2005.

[13] U. Onunkwo, Y. Li, A. Swami, "Effect of timing jitter on OFDM-based UWB systems," *IEEE Journal on Selected Areas in Communications*, vol. 24, no. 4, pp 787–793, April 2006.